Population Coding for Neuromorphic Hardware

Khan, SQ, Ghani, A & Khurram, M

Original citation & hyperlink:
Khan, SQ, Ghani, A & Khurram, M 2017, 'Population Coding for Neuromorphic Hardware' *Neurocomputing*, vol 239, pp. 153-164
https://dx.doi.org/10.1016/j.neucom.2017.02.013

DOI 10.1016/j.neucom.2017.02.013
ISSN 0925-2312

Publisher: Elsevier

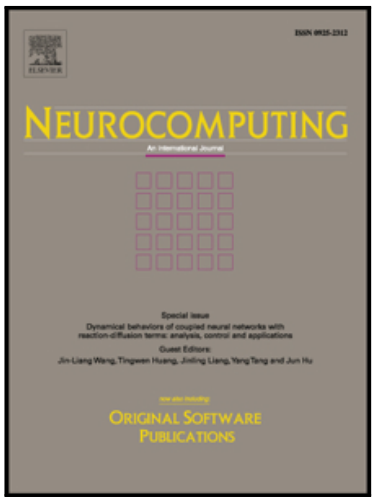

Population Coding for Neuromorphic Hardware

Saad Qasim Khan , Arfan Ghani , Muhammad Khurram

PII: S0925-2312(17)30283-7
DOI: 10.1016/j.neucom.2017.02.013
Reference: NEUCOM 18079

To appear in: *Neurocomputing*

Received date: 21 July 2016
Revised date: 5 January 2017
Accepted date: 5 February 2017

Please cite this article as: Saad Qasim Khan , Arfan Ghani , Muhammad Khurram , Population Coding for Neuromorphic Hardware, *Neurocomputing* (2017), doi: 10.1016/j.neucom.2017.02.013

Population Coding for Neuromorphic Hardware

Saad Qasim Khan[¥], Arfan Ghani [Ψ] and Muhammad Khurram[¥]
[¥]Dept. of Computer & Information Systems Engineering
NED University of Engineering & Technology
Karachi, Pakistan
[Ψ] Dept. of Electrical and Electronic Engineering
Coventry University, Coventry CV1 5FB
United Kingdom
{saadqasimkhan, mkhurram}@neduet.edu.pk
A.Ghani@Coventry.ac.uk

Abstract— Population coding has been established as the key mechanism for decoding sensory information received from periphery organs such as retinas and cochlear. In this paper a novel architecture is presented to embed population coding in neuromorphic hardware. A resonance based mechanism between two layers of neuron is utilised in the presented work. The mechanism discussed in this paper facilitates selective triggering of higher layer neurons which serves as target ensemble for evaluation of a particular input of interest. It has been shown that presented model can be used to detect any physical quantity (light intensity, temperature, etc) feed to the sensor on the basis of population coding.

Keywords- Population Coding; Neuromorphic Hardware; Synaptic Plasticity; Interspike Interval; Tuning Curve

I. INTRODUCTION

The main idea of Neuromorphic Hardware was conceived by Carver Mead in late 1980's [1]. The idea was basically centered at implementation of nervous system on Very Large Scale Integration (VLSI) hardware. Since then a number of neuromorphic hardware solutions have been presented [2-10] by different research groups. Neuromorphic hardware design is being considered by many processor design industry giants such as Intel, HP and Qualcomm as the solution for next generation computing demands. Intel has recently revealed their Spin-lateral valve based neuromorphic hardware [11]. HP is eagerly pursuing with their memristor based neuromorphic hardware [12], Qualcomm is also working in the same direction [13]. This trend clearly indicates the growing interest around the world to pursue with neuromorphic hardware designs as the solution for next generation computational devices. As the transistor dimension is shrinking to submicron level, there are more nonlinearities that incorporate into the transistor operation thus making its response unreliable and random [14].

In the past, few research groups have also presented their indigenous neuromorphic hardware designs such as FACET [7], SpiNNaker [8] and a VLSI model presented by research group at ETH Zurich [3]. There is one commonality in all these neuromorphic design approaches that all these hardware designs emphasize on time domain techniques to embed plasticity within neuromorphic hardware. One of the prominent time domain techniques for plasticity is the Spike Time Dependent Plasticity (STDP) [15, 16] which provides a mechanism to embed plasticity in neuromorphic hardware. STDP provides a window function to decide on the correlation of spikes generated by the pre-synaptic and the post-synaptic neuron. The correlation window on the basis of correlation between the spikes from the presynaptic and postsynaptic neuron, updates the conductance value *g*. The conductance value *g* is used to represent the strength of connection between any two neurons. The learning algorithms implemented by these hardware are similar to the one defined within Artificial Neural Network (ANN) theory [17]. To the best of author's knowledge, there exists no ANN model which provides support to embed population coding in a network structure. In this paper a different approach is adopted to model synaptic connection. Rather than considering a variable conductance value *g*, a bandpass filter is realized as a synaptic connection which implements variable conductance in frequency domain.

It has been established through numerous neurophysiological studies [18-21] that population coding is the mechanism behind decoding of sensory information from periphery organs. Individual neuron response is considered as noisy [22] whereas neuronal ensemble response provides more reliable results for true perception of sensory data. Population coding is witnessed in different regions of cortex which includes primary visual cortex [23], motor cortex [24], wind sensor of cricket [25] and other related areas [26]. On the basis of above evidences it can be stated that nearly all cortical sub-regions designated for decoding different sensory information employs population coding for evaluation of information present in the environment. Implementation of bio-inspired population coding in neuromorphic hardware requires a network based on spiking neurons.

Spiking nature of neurons makes it a complex dynamical structure as reported by Hodgkin and Huxley [27]. The dynamical nature of a neuron characterizes spiking output from it. Two prominent spiking modes are the tonic spiking mode and the burst mode [28]. Both modes of spiking do encode the information that one neuron is trying to pass to the succeeding layer of neurons by varying Inter-spike Interval (ISI) of the output spikes. ISI [29] has become a

standard for neuronal information code that is transmitted between different layers of neurons. The ISI which is normally represented in time scale can be converted to frequency value for analysis of information transmitted by the neuron in frequency domain.

The model proposed through this paper describes a population coding mechanism for neuromorphic hardware. The proposed model has the advantage of using minimal resources for implementation of a network that embeds population coding. The presented model decodes the stimulus through distinct response of the postsynaptic population. One of the limitations of the presented model is the use of passive bandpass filter which marginally attenuates the passband frequency. This paper is summarized as follows: Section II provides insight into neurophysiological aspects of population coding; population coding by Direction Selectivity (DS) neurons in primary visual cortex [23] has been analyzed as test case. Section III describes the existing techniques to embed population coding on neuromorphic hardware. Trainable Analogue Block (TAB) framework [30] has been briefly discussed in this section as being the only contestant to embed population coding on neuromorphic hardware. Section IV presents a novel resonance based synaptic connection for neuromorphic hardware. This artificial synapse facilitates selective triggering on the basis of spiking output frequency by the presynaptic neuron. The concept of selective triggering is also discussed in the same section. Section V discusses the building block for the network model presented in this paper. Section VI discusses the network dynamics and its role in embedding population coding in neuromorphic hardware. Section VII provides the implementation for the proposed network. Section VIII gives the conclusion.

II. NEURAL POPULATION CODING

Population Coding is the key mechanism for decoding sensory information that represents physical quantities such as direction of a visual stimuli, orientation and auditory stimuli. A perception regarding any physical entity described above is generated by a cluster of neurons. The sensory information is passed to a single neuron that is responsible to encode the stimulus in terms of output spiking rate. There are two predominant neuronal encoding techniques namely rate-encoding and temporal-encoding. In this paper rate-encoding mechanism is adopted for encoding stimuli feed to a neuron. The relationship between input stimulus strength and the output spiking rate is governed by the dynamical properties of the encoding neuron [31]. On the basis of dynamical behavior exhibited by the neurons, they can be classified into three categories as originally proposed by Hodgkin-Huxley [27] which are Class I, Class II and Class III excitable neurons. The characteristic curve of Class I excitable neuron is depicted in Fig. 1 from which it is evident that there exist a static relationship between stimuli which is current in this case (given in *pA*) and the output asymptotic firing rate (given in *Hz*). To be more accurate it is better to say that the input stimuli and the output spiking frequency have a sub-linear relationship which can be represented as

$$h(i) = a_0 + C(1-exp(-i)) \quad (1)$$

Here $h(i)$ is a function of stimuli current i, representing asymptotic output spiking rate, C is the adjustment parameter and a_0 is the shift from the origin. By applying the above stated expression, a similar sub-linear curve is obtained as shown in Fig. 1 which serves as the characteristic curve for Class I excitable neuron. Since Class I excitable neurons are utilized in this work, the discussion will be restrained to Class I neurons only. The characteristics of Class II and Class III excitable neurons are out of the scope of current work. For details regarding Class II and III excitable neurons one may refer to the detailed analysis carried out by Izhikevich [31].

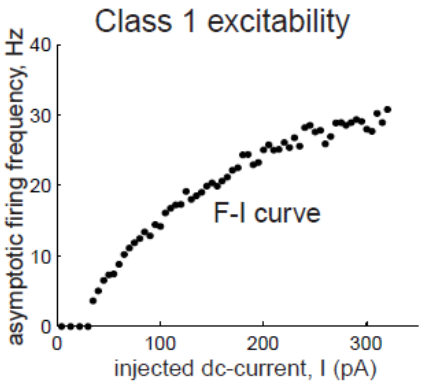

Figure 1. Characteristic curve for Class I excitable neuron. This picture is adopted from [31]. It indicates the transfer function of Class I neuron that is to convert injected current (in *pA*) into output spiking frequency (in *Hz*).

This coded information in terms of spiking frequency is passed to the respective cluster of neurons. The same cluster of neurons is responsible for decoding the information to create a correct perception about an event present in the environment. As an example of this decoding, we have considered a constrained application of visual cortex which is inspired by the Direction Selectivity (DS) neurons from primary visual cortex [23]. Consider that the neurons have the capability to decode the motion of visual stimulus in 2-dimensional space. The 2-dimensional space distribution is depicted in Fig. 2.

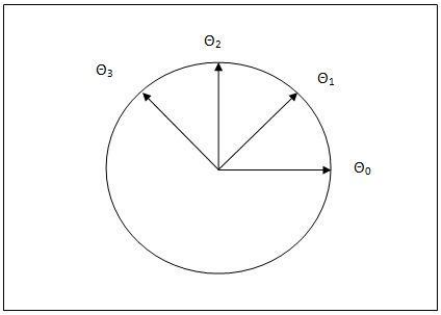

Figure 2. A 2-dimensional space distribution for direction selectivity between 0 and 0.8π. Four distinct directions are identified for decoding by four neurons in target population

The 2-dimensional space shown above is distributed into four possible directions. The value of θ is parameterized between 0 to 0.8π range. In order to realize a population able to decode the motion within these directions, a vector of four neurons has been realized.

$$N = \{ n_0, n_1, n_2, n_3 \} \quad (2)$$

Here n_i represents individual neuron within a population. It has been assumed that each neuron has distinct tuning curve with distinct preferred direction. Each neuron within a given population has a characteristic tuning curve that represents its response to the range of possible stimuli applied to the network [32]. A simple approximation for a tuning curve can be of a Guassian curve as depicted in Fig 3. The stimulus *x* can be voltage or current value (direction is encoded within this value) which is transferred from the sensory neuron to the population. The response along the vertical axis is the number of spikes generated per unit time and the peak response represents the preferred direction for individual neuron.

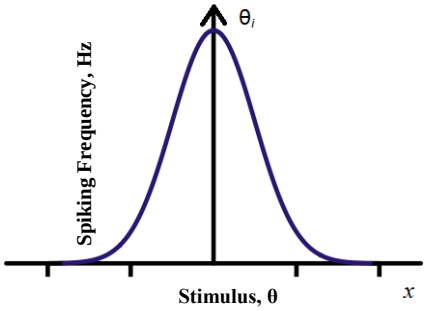

Figure 3. Tuning curve for an individual neuron. The x-axis represents sensory stimuli, θ and y-axis represents neuronal response for range of stimuli. This is generalized representation of tuning curve therefore exact scaling values are not mentioned.

The tuning curve depicted in Fig. 3, is an approximation of tuning curve as a Guassian function, $f_i(s)$. The expression to represent the Guassian function [20] is expressed as follows:

$$f_i(s) = ke^{-(s-s_i)^2/2\sigma^2} \quad (3)$$

In Eq. 3, $f_i(s)$ is the average response of the postsynaptic neuron which forms the tuning curve for that particular neuron. The tuning curve is a function of encoded variable *s* (the direction θ in this particular case) and s_i is the preferred direction of that neuron. Here σ is the width of the tuning curve, $s - s_i$ is the angular difference for each tuning curve and *k* is the adjustment parameter.

It can be stated that each neuron n_i in the population has the preferred direction θ_i plotted in Fig 2. The tuning curves for the population of four neurons with distinct preferred directions are depicted in Fig 4. Here overlapping of tuning curve between the neighboring neurons is a possibility but each neuron do have a distinct peak response which indicates the preferred direction θ_i for individual neuron n_i.

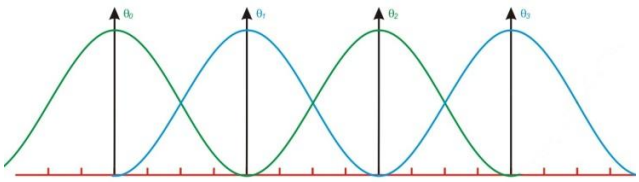

Figure 4. Tuning curves of four neurons in a population with distinct preferred directions, θ_i. Each neuron decoding the value of θ_i in terms of its maximal output response.

The vector for all preferred directions can be represented as

$$\Theta = \{ \theta_0, \theta_1, \theta_2, \theta_3 \} \quad (4)$$

If the response of the i^{th} neuron can be characterized by a nonnegative integer r_i then the response vector may be expressed as

$$R = \{ r_0, r_1, r_2, r_3 \} \qquad r \in \mathbb{R} \quad (5)$$

Here r_i represents the response for the n_i neuron. If response of the neuronal population is considered as a weight value then Eq. 4 and 5 can be combined together to represent the weighted response of individual directions as

$$I = \{ r_0\theta_0, r_1\theta_1, r_2\theta_2, r_3\theta_3, r_4\theta_4 \} \quad (6)$$

Here *I* represent the information that is contained within a neuronal response of a population regarding direction of a visual stimulus. The mean information value will remain same for motions in each different direction.

One important aspect of above mentioned population coding mechanism is the robustness of model against random noise. Any signal feed from sensor such as θ may contain noise. The value for θ may be expressed as

$$\theta_i^* = \theta_i + e^* \quad (7)$$

In Eq. (7), θ_i represents actual stimulus whereas e^* represents random noise added to the signal. In Fig. 4 each preferred direction of a neuron has a constant distance with the preferred direction of adjacent neuron which may be represented as *d*. For misclassification of applied stimulus θ_i as θ_j, the noise value must fulfill the following constraint.

$$e^* \geq d/2 \quad (8)$$

If noise fulfills the above constraint, neuron with preferred direction of θ_j will be triggered instead of neuron with preferred direction θ_i. In this case, the actual stimulus θ_i

which was applied to the sensor will be misclassified as θ_j by the target population. If value of e^* is equal to $d/2$ such as $(1/2)*d$ then both adjacent neurons will be triggered (the intersection point between the two tuning curves in Fig. 4) with averaged frequency. The value of e^* must be large if d is large, following the constraint in Eq. 8. This represents that large d will result in an accurate classification due to large constraint on e^* whereas small d will result in an approximate classification due to smaller constraint on e^*.

Traditionally, in neurophysiological studies of population codes different statistical tools were utilized which includes Maximum Likelihood Estimator (MLE) [33], Fisher Information [34], Chernoff distance measure [35]. All these tools were employed to evaluate the response of a population for a particular stimulus applied.

MLE is the most extensively employed tool for evaluating the response of a population when presented with stimulus of interest. The main reason for its popularity among the neurophysiological research community is for being the optimal discriminator with an error value of $1/\sqrt{N}$ where N represents the number of neurons within a population.

Fisher information is basically employed to measure the estimation error of a continuous variable. In the scenario of population coding it is used to represent the error in estimating the stimulus value applied to presynaptic neuron and decoded by the postsynaptic neurons.

Chernoff distance is used as a measure of stimuli discrimination capability for a population of neurons. Chernoff distance measures the difference between two distributions. These distributions may be referred as the distinct response of neurons when presented with the same stimuli based on distinct tuning curve preferences. Let $P(r|\theta_i)$ represents the response of neuron r when presented with stimulus θ_i. Then Chernoff distance $D_c(\theta_1, \theta_2)$ can be represented as

$$D_C(\theta_1, \theta_2) = -\log Tr_{\vec{r}} P^{\alpha}(\vec{r}|\theta_1) P^{1-\alpha}(\vec{r}|\theta_2) \quad (9)$$

$$D_C(\theta_1, \theta_2) = \max_{\alpha} D_{\alpha}(\theta_1, \theta_2) \quad (10)$$

Here $D_c(\theta_1, \theta_2)$ is the maximum value of $D_\alpha(\theta_1, \theta_2)$ in terms of α and the value of α is in between the range of 0 and 1.

III. EXISTING MODELS FOR POPULATION CODING

The only proposed solution to embed population coding on neuromorphic hardware, to the best of author's knowledge is Trainable Analog Block (TAB) framework [30]. The TAB employs Linear Solutions of Higher Dimensional Interlayers (LSHDI) framework. It has been assumed that LSHDI principle is similar to neural population coding. LSHDI was previously employed for Functional-Link net computing [36]. Other variants of LSHDI [37, 38] for neural computing have also been proposed in the past. The Neural Engineering Framework (NEF) [39], which is a popular framework for spike based computation in the neuromorphic hardware design community, is also based on the same LSHDI principle.

LSHDI is a three layered feed forward network [40] shown in Fig. 5. The three layered network comprises of input, hidden and output layers. The neurons in the hidden layer are much larger in number as compared to the input layer, with nonlinear transfer functions. In order to embed variability in the hidden layer response, their connections with the input layer are randomly generated and maintained throughout the training period. The lower dimensional input is mapped onto higher dimensional hidden layer space. The nonlinearity of hidden layer neurons facilitates classification of input space data on a hyper plane formed by the hidden layer. The weight values are determined by the product of inverse layer activations with the desired output value.

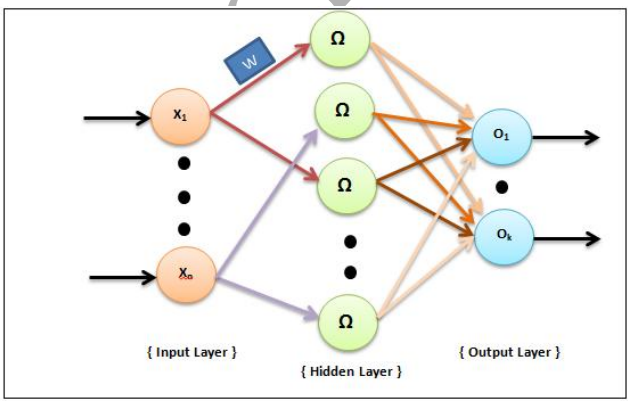

Figure 5. LSHDI principle network. Each link has an associated weight value which is only depicted with one link (for the sake of compactness) between the input neuron X1 and first hidden layer neuron marked as W. Input layer has N neurons labeled as X_1-X_n. There are M number of hidden layer neurons which are labeled as Ω to represent nonlinear sigmoidal activation function. Here $M >> N$ for LSHDI based network. The last layer represents output layer labeled as O_1-O_k having K number of neurons in output layer as required by the application.

In order to embed variability in the input layer response for presented stimulus, TAB framework exploits the variability of transistors at the submicron fabrication level. Random device mismatch is a desirable feature for TAB framework. The heterogeneity of tuning curve which is desirable feature to embed population coding in any structure is again employed with the help of device mismatch. The main application that is achieved through this architecture is the regression task that is employed to approximate some nonlinear functions such as sine, cube and sinc function.

Despite of all the evidences provided in the TAB framework based cell to embed population coding, there are some major concerns to address for designing a model that embed population coding in its true spirit.

- LSHDI framework utilizes a large number of nonlinear hidden layer neurons as compared to the input layer. There is no proportion identified

between the number of hidden layer neurons and the input layer neurons to properly approximate any nonlinear function. Large number of hidden layer neurons puts an additional space requirement on the hardware.

- The device mismatch is beyond the control of designer. It is not obvious as how it is possible to apply any deterministic rule on the TAB framework? Each device fabricated may differ in their behaviour. It is nearly impossible to define any deterministic framework for designing application. In order to control device variation, a systematic offset is provided. There is major calibration effort required to assess the offset value given proper data regarding variation in individual TAB module.
- There is no reference to population vector in the said work. Population vector is the major part of any population coding mechanism. Rather than discussing population coding authors presented typical application of neural networks as an approximator of nonlinear functions.
- Only a single TAB framework based cell is discussed. The network response is not evaluated in the said work.

On the ground of above mentioned drawbacks in the previously stated work on population coding, we have tried to address all these issues in the current work with a different approach. For details, view section VI that addresses network dynamics.

IV. RESONANCE BASED SYNAPSE

In the past couple of decades there were number of evidences presented [41, 42] that shows that synaptic junctions which exhibit short term potentiation and depression perform bandpass filtering on the output from presynaptic neuron.

Many neurons fire bursts to encode information and transmit it to the succeeding layer of neurons. A burst may be defined as closely spaced stereotypical spikes. The spikes have a typical feature of 100 mV amplitude and duration of 1 millisecond [31]. The feature that varies to embed information is the ISI. Different bursts are generated with different ISIs. It is considered that the burst are more reliable way of communication between neurons than individual spikes [42]. It is also suggested that the postsynaptic response may depend on the frequency content of the burst due to a preference of a particular resonance at the synaptic and the neuronal level.

The transmission of signals from presynaptic neuron to the postsynaptic neuron is thought to be more effective when the presynaptic neuron fires burst with a particular resonance that is formed by the ISI between individual spikes of a burst [44]. It is also considered that different postsynaptic neurons have different resonant frequency which makes burst with a particular ISI, resonant for one postsynaptic neuron while non-resonant for the other postsynaptic neurons.

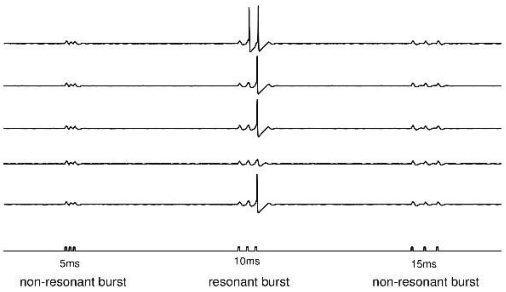

Figure 6. Experimental obesrvations form mesencephalic V neurons in brainstem [43], showing selective resonance with a burst of 10 ms. Each vertical stream represents the response of a single neuron at different time instances except for bottom stream which represents exitatory input in terms of callibrated input bursts.

As shown in Fig. 6, the neurons in brainstem are resonant to a 10ms burst while non-resonant to any burst that has a ±5ms difference from the resonant burst. This is indicative of how neurons transmit information selectively to a particular set of neurons by varying the ISI of burst generated.

It has been established through numerous neurophysiological studies [44-47] that short-term synaptic plasticity contributes to temporal filtering of synaptic transmission. Depression acts as low-pass filter whereas facilitation acts as high-pass filter. Therefore synapses capable of exhibiting both characteristics of depression and facilitation acts as a bandpass filter [44].

In Fig. 7 synaptic junction is shown in different modes of operation which includes short-term depression as lowpass filter, facilitation as highpass filter and both short-term depression and facilitation as band-pass filter with a peak response that represents the resonant frequency. Through above discussion, it has been established that the synaptic junction perform band-pass filtering operation on the output from presynaptic neuron. This bandpass filtering facilitates selective triggering of neurons at the postsynaptic side based on the resonance feature of burst generated by the presynaptic neuron.

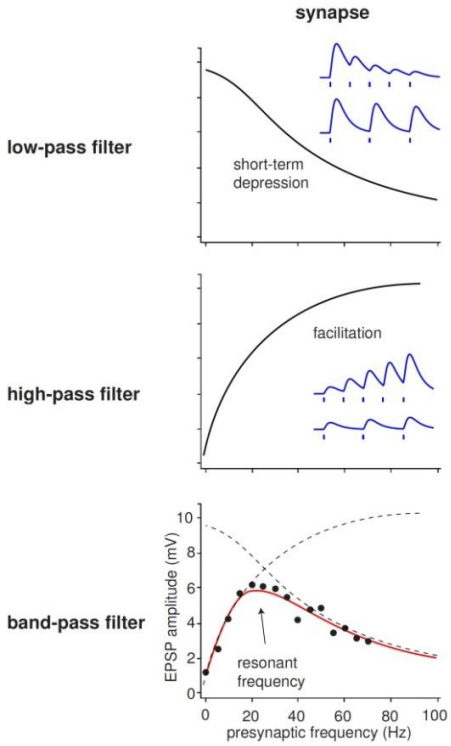

Figure 7. Filtering operation performed by a synaptic junction [44]. All three graphs share the same x and y-axis scaling. Top most graph shows response of a synapse for short-term depression, The middle graph shows synaptic operation in facilitation and bottom graph shows synapse exhibiting both short-term depression and facilitation.

V. BUILDING BLOCKS OF PROPOSED NETWORK

Before discussing complete network model it is beneficial to discuss the subparts associated with the network model. The most important element in the network is the neuron model. The neuron model utilised in this work is discussed in detail in following section *A*. Few requirements associated with the neuron model are that it follows the rate encoding characteristic of Class I neuron discussed previously. Apart from following the basic rate encoding characteristic, it offers a compact and stand-alone model of neuron without inclusion of external bias voltages. After neuron model, the synaptic connection is discussed in section *B*. The synaptic connection initially utilizes a simple first-order Butterworth passive bandpass filter [48]. As a requirement from synaptic connection transfer function is that it doesn't overlap or have minimal overlapping with the transfer function of other synaptic connections so that one value of stimulus applied to presynaptic neuron can properly be identified from other values. Section *C* describes a current integrator circuit that is responsible to convert the sinusoidal wave that is output from the bandpass filter into voltage value that can be applied to the postsynaptic neuron. This current integrator circuit is realized as a dendrite part of post synaptic neuron. Section *D* discusses the complete network model which includes all the subparts discussed in above three sections.

A. Neuron Model

In this work an accelerated capacitor-less model for Class I excitable neuron with static threshold value is utilised. The model adopted as a neuron is a current starved ring oscillator, normally employed as Voltage Controlled Oscillator (VCO) [49] in mixed signal circuits. The neuron model has the capability to encode the stimulus applied to the neuron in terms of output frequency. The model presented is a compact neuron model as it utilises only seven transistors and has no capacitor in the feedback path. The external capacitors may put an additional requirement for space and also considered as the main factor in dynamic power dissipation. The capacitors may induce the time constant that is witnessed in biological neurons. The capacitors were included in the conventional Axon Hillock [1] neuron model for matching the time constant of biological neurons. The exclusion of capacitor from the model lowers down the dynamic power dissipation from the Complementary Metal-Oxide Semiconductor (CMOS) circuitry. The presented model utilizes a ring oscillator comprising of only seven transistors, for generating tonic spikes in the context of neuromorphic hardware. The following Fig. 8 shows the neuron model.

Same neuron model is used to design presynaptic and postsynaptic neurons. The complete network is based on rate-encoding neurons shown in Fig. 8. The neuron model takes Direct-Current (DC) value as input and provides oscillations at the output port that are proportional to the applied DC value. The neuron model functions in the strong-inversion domain. In contrast to the biological time-scale of neurons, it operates on accelerated time scale. Thus this model is considered as an accelerated silicon neuron model.

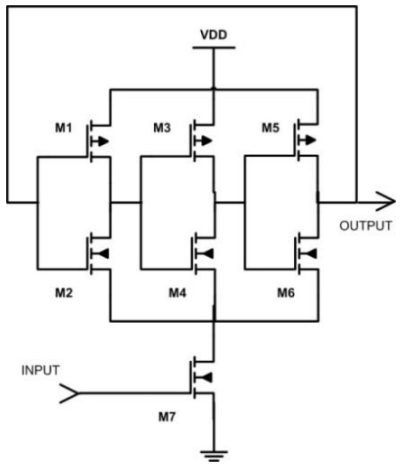

Figure 8. Circuit diagram of current starved Voltage Controlled Oscillator (VCO) utilized as Class I excitable neuron. The proposed model is capable of encoding input in terms of output spiking rate with a fixed threshold.

The valid operating region for the presented model is the window of values for applied gate voltage where transistor (M7) operates in the triode region. In cutoff region, the output waveform is not considered as a valid output wave whereas in saturation region, there is no further change in the output despite of increasing the input value. The only region of interest is when the NMOS transistor *M7* acts as a voltage controlled resistor. The standard expression of a transistor's drain current operating in triode region is as under;

$$I_D = k_n\left[(V_{in} - V_T)V_{DS} - \frac{V_{DS}^2}{2}\right] \quad (11)$$

Where $V_{in} = V_{GS}$ for the presented model and V_{in} refers to the stimulus input which is voltage for controlling an NMOS that acts as a Voltage-Controlled-Current-Source (VCCS) in the given model. Further in the above expression k_n represents the gain factor of transistor, V_{DS} represents the potential drop between source and drain of a transistor and V_T represents threshold voltage.

The circuit model presented here is simulated using Multisim software. The NMOS model selected for simulation is generic 2N6659 with TO-39 footprint whereas PMOS model is Single P-Channel Hi-Rel MOSFET 2N6804 with TO-204AA footprint. The relationship between the input value (in *volts*) against the output frequency (in *MHz*) can be represented with a plot as shown in Fig. 9.

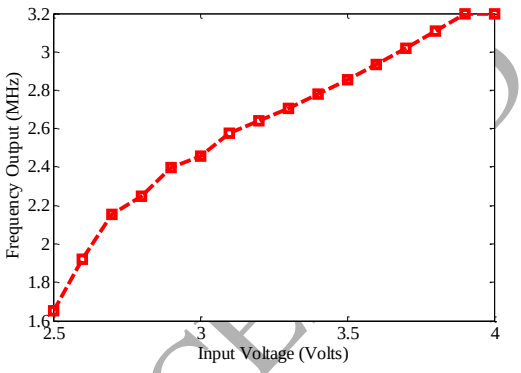

Figure 9. The voltage-frequency curve for poposed neuron model

It is evident from the plot depicted in Fig. 9 that the presented model has the capability to encode the stimulus input in terms of output spiking frequency. The plot is scaled from 2.5 V which serves as the threshold value for a neuron to enter into spiking mode. The plot shown in Fig. 9 has striking resemblance with the *f-I* characteristic curve for Class I excitable neuron shown in Fig. 1. The main difference between the proposed neuron model and biological counterpart is the accelerated timescale of the proposed model. Recently there are number of accelerated neuron models proposed [5]. The same approach is adopted for the proposed neuron model. Accelerated models have advantage of lower latency and it consumes less area on silicon real state. The reduction in the silicon area is due to lower impedance requirement of circuits operating at higher frequencies.

The time domain response of the neuron with two distinct input values that is V_{in} = 2.5V and V_{in} = 3V is shown in Figure 10(a) and 10(b) respectively.

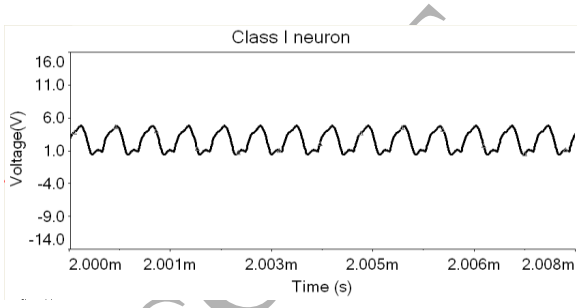

(a)

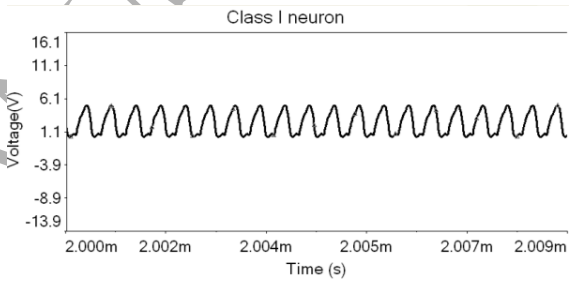

(b)

Figure 10. (a) Output with input V_{in} = 2.5V (b) V_{in} = 3.0V

The proposed neuron model is a standalone rate neuron model similar to Axon-Hillock neuron [1] but with much lesser area requirement and power consumption. Further it does not require external parameters (control voltages) for calibration. The proposed model can easily be employed as Class I excitable neuron in neuromorphic hardware.

B. Synaptic Connection

As discussed is Section *IV*, synaptic connections that exhibit short term potentiation and depression act as band-pass filters, a synaptic connection is considered as a band-pass filter in this paper. Simple *RLC* circuit is utilised to design a passive 2nd order band-pass filter.

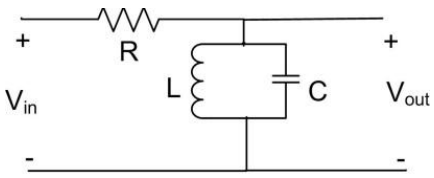

Figure 11. RLC based 2nd order bandpass filter

The *LC* tank is basically responsible to provide a resonent frequency for the filter. The resonent frequency for the filter can be expresed as

$$f = 1/(2\pi\sqrt{(LC)}) \quad (12)$$

This resonant frequency may be considered as the passband frequency for bandpass filter allowing only one frequency and attenuating all other stopband frequencies. The transfer function can be represented with a bell shaped curve for the bandpass filter as shown in Fig. 12.

Here ω value represents the resonant frequency in rad/s. The ω term is directly replaceable in Eq. 12 by considering $\omega = 2\pi f$. There are two cutoff frequency points represented by -3 dB points. The lower cutoff frequency point is also marked as ω_l and higher cutoff frequency point marked as ω_h. The bandwidth of the filter can be represented as $\omega_0 = \omega_h - \omega_l$.

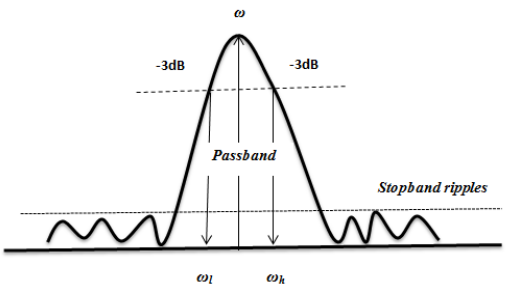

Figure 12. Frequency domain representation for transfer function of a bandpass filter. Here x-axis represents frequency spectrum and y-axis represents magnitude response of the filter.

Here $\omega_a = \omega/\omega_0$. The smaller value of ω_a increase the quality of a filter. The quality of the filter can be inceased by increasing the order of the filter. The transfer function of n^{th} order butterworth filter is represented as

$$H(\omega) = \frac{1}{1 + \left(\frac{\omega}{\omega_0}\right)^{2n}} \quad (13)$$

Another interesting fact from the above frequency response of the bandpass filter shown in Fig. 12, is the resemblance between the tuning curve (depicted in Fig. 3) and the transfer function of the bandpass filter. The transfer function of a bandpass filter can be approximated as sigmoidal function as represented by Eq. 3. In this paper another important assumption is the consideration of tuning curve as the function of selective filtering by the synaptic connections rather than a nonlinear function of postsynaptic neurons. This hypothesis facilitates the implementation of tuning curve in electronic hardware without employing a hidden layer of nonlinear neurons. This implementation can be carried out by employing bandpass filters as synaptic connections as was done in the presented work.

C. Dendritic Connection

The key requirement from dendritic connections is to convert output from the synaptic connection into a value that can be feed to a postsynaptic Class I excitable neuron. The output from the synaptic connection that is a bandpass filter is a periodic wave having variable frequency values as shown in Fig. 10. The input requirement for a neuron model is a DC voltage value that is applied at the fan-in of a neuron. For this purpose, we employ a current integrator circuit to convert the output from the synaptic connection into a DC voltage value that can be feed as an input to the postsynaptic neuron. The simple electronic circuit for the current integrator circuit is shown in Fig. 13.

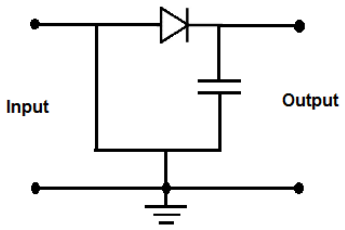

Figure 13. Dendritic connection

The current integrator comprises of a diode to eliminate negative cycles from the input wave, half wave rectification and a capacitor for current integration at the output node. This simple circuit serves the purpose of dendritic connection for postsynaptic neuron in the network model presented here. Although employing a diode in the path will result in *0.7V* drop but the impact will be negligible as far as output from integrator block is concerned.

VI. NETWORK DYNAMICS

The complete network picture is depicted in Fig 14. A network of 1-to-4 neurons is considered for embedding population coding in neuromorphic hardware. At the left side of the network, a single neuron is interfaced with the sensor node that passes stimulus information in terms of DC value to the presynaptic neuron. If the value is above threshold V_T

then the neuron will start oscillating according to the voltage applied.

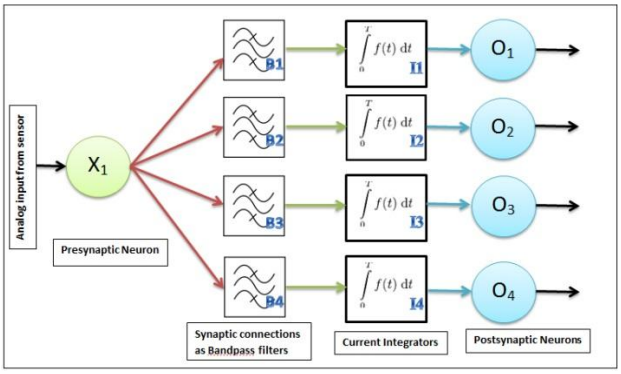

Figure 14. Network diagram of the proposed population coding for 1-to-4 network.

Here a network of 1-to-4 neurons is considered in connection to the population vector discussed in section *II*, that has the capability to decode four different directions embedded in the response of the ensemble neurons. Similarly, the proposed network has the capability to decode the stimulus in terms of neuronal ensemble response. Thus the population vector for this network has four neurons in its population vector. However the network model can be extended to have more neurons and thus more representation.

$$N = \{O_1, O_2, O_3, O_4\} \quad (14)$$

The network comprises of a single presynaptic neuron that is interfaced with the sensor. The sensor passes continuous-time analogue value to presynaptic neuron. Normal real-time sensors provide analogue values thus any sensor can be directly interfaced with the network model. Only requirement from this sensor to neuron interface is to normalize the voltage value between the operational range of neuron model described in this work. Details regarding this operational range are provided in previous section *V.A* .

The presynaptic neuron following the characteristic curve shown in Fig. 9 in section *V.A*, encodes the applied stimulus in terms of spiking output frequency. This spiking output is transmitted through all the fan-outs of a presynaptic neuron to the succeeding layer of bandpass filters, labeled as *B1-B4* in Fig. 14, treated as synaptic junctions in this work. The bandpass filters transmit only one distinct spiking frequency through them, blocking all other frequencies. Since the information regarding the stimulus is encoded in terms of spiking frequency, it can be stated that the information regarding only unique value of applied stimulus feed to presynaptic neuron and encoded in terms of distinct spiking frequency, is transmitted across the synaptic junction that is a bandpass filter in this case.

The output of the bandpass filter is feed to a current integrator. The current integrator block, labeled as *I1-I4* in Fig. 14, will convert the sinusoidal output from bandpass filter into a DC value that can be feed to the postsynaptic neuron. The sinusoidal wave cannot be directly applied to fan-in of a Class I neuron model shown in Fig. 8. Thus integrator block acts as a frequency to voltage converter. After the stage of current integration, there is an array of postsynaptic neurons, O_1-O_4. These neurons can be considered as the target ensemble to decode the information passed from the sensor attached to the network.

A. Selectrive Triggering of Postsynaptic Neurons

It is possible to perform selective triggering of postsynaptic neurons by using this model. The proposed model offers distinctive advantages because no additional hardware is required for Winners Take All (WTA) circuitry. To the best of author's knowledge, no other model offers this advantage. WTA is the prominent algorithm for neuromorphic applications [50]. WTA performs the same task of selecting a winner node from all the competing nodes. WTA in this manner can be considered as an algorithm that do perform selective triggering of post synaptic neurons, which is an inherent capability of the proposed network model based on resonance based plasticity mechanism. The proposed network also selects a winner node by selectively triggering it for the stimulus that is applied to the presynaptic neuron. WTA has been utilised in neuromorphic hardware to achieve variety of task which includes, Dynamic neural fields [51], selective attention [52], optic flow measurement [53], etc.

B. Tuning Curve as a function of synaptic selectivity

In conventional neuroscience theory, tuning curve is considered as a function of postsynaptic neurons [18-22]. In this paper we have demonstrated that the tuning curve can be considered as function of synaptic selectivity to output spiking frequency. The response of the postsynaptic neurons that is represented with the help of a tuning curve can be considered as the projection of transfer function of bandpass filtering performed by the synaptic connections. The characteristic expression for tuning curve can also be expressed as

$$f(\theta) = \begin{cases} f_{min} + (f_{max} - f_{min}) cos^m\left(\frac{\pi\theta}{2a}\right) & , |\theta| < a \\ f_{min} & , otherwise \end{cases} \quad (15)$$

In the above expression, the tuning curve is represented as a function of output spiking frequency by postsynaptic neuron.

C. Population vector calculation

The population vector employed in this work is expressed in Eq. 16. In order to understand the population coding mechanism, consider that the sensor provides information about physical entity in terms of DC voltage value as depicted in Fig. 15. This staircase representation of voltage values represent four distinct value of a physical quantity, such as direction of motion, read by the sensor. This voltage value provided by the sensor is applied to presynaptic neuron that is directly interfaced with the sensor node.

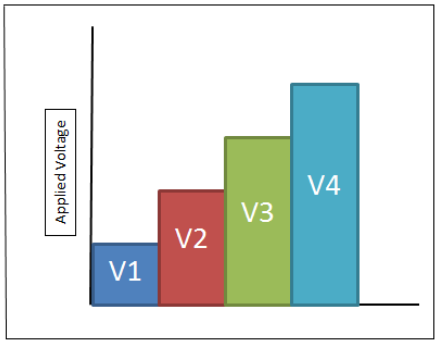

Figure 15. Four different votage values read by the sensor

The population vector is required to properly identify a stimulus applied to presynaptic neuron. It has been assumed here that the sensor has the capability to pass the direction of motion in terms of different voltage values. The four different direction of motion can be expressed as shown in Fig. 16. The direction of motion is encoded in terms of voltage value passed by the sensor to the presynaptic neuron. Voltage value *V1* is used to represent motion of a visual stimulus along the horizontal axis with $\theta_1 = 0$ degree. Subsequently θ_n will be represented by the voltage value V_n.

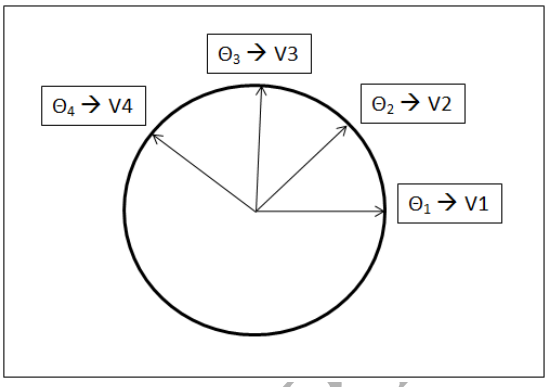

Figure 16. Directional chart in the 2-dimensional space

The DC value applied to the presynaptic neuron enforce the neuron to oscillate with a particular frequency as previously discussed in section *V.A*. The information that was initially transmitted by the sensor node is then encoded in terms of spiking frequency by the presynaptic neuron. The output from the presynaptic neuron is transmitted to all the synaptic junctions. On the basis of frequency selective transfer function embedded by the synaptic junctions, a particular frequency through one or more synaptic junctions is transmitted to the next stage of current integrator. The current integrator converts the sinusoidal output into DC value that is feasible to be applied to a postsynaptic neuron. The postsynaptic neuron that receives a DC value that is above threshold, triggers. This triggering by a single postsynaptic neuron can be represented as a binary '1' in the population vector whereas neurons that doesn't trigger to the applied stimulus can be represented by a binary '0'. The population vector can therefore be expressed as

$$N = \{0, 0, 1, 0\}. \quad (16)$$

The population vector expressed in the above expression indicates that for the stimulus presented to the presynaptic neuron only the third neuron will trigger thus conveying the information about stimulus in terms of neuronal population response. It indicates that θ_3 is the direction detected by the sensor node. The processing through each synaptic connection can be summarized by the following flow-chart that depicts the complete processing chain from sensor to triggering of target neuron in a population.

.

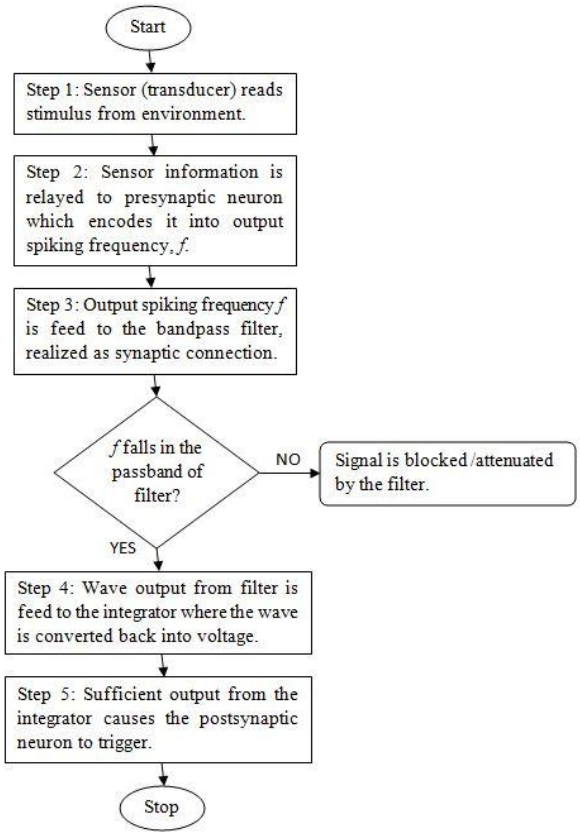

Figure 17. Processing through single synaptic connection

VII. IMPLEMENTATION

In this section, the physical implementation of the proposed network is presented. The wiroboard experiments were carried out for the proposed network model. In order to realize the circuit for neuron shown in Fig 8, an inverter IC 7404 is utilized. IC 7404 offers six inverters from which three inverters are utilized to form a ring oscillator. The ground pin of the IC is connected to an NMOS transistor (device number 2N7000). This configuration generates the

neuron circuit model depicted in Fig 8. The gate of the NMOS transistor *M7* is connected to a 5K rheostat. Here we assumed that a 5K rheostat can be used to model any sensor node. The rheostat is connected between 5V (V_{DD}) and ground. The rheostat is therefore calibrated to provide values from 0-5V DC. The desired operation required by the NMOS is to work as voltage controlled resistor in its triode region of operation. The NMOS also provides a fixed threshold value (1.5V), which is a requirement for rate neuron model. The triode region of operation for the said NMOS is 1.5-2V. Within this region of operation we get the voltage-controlled oscillator behaviour from the neuron circuit which is equivalent to the behaviour of Class I excitable neuron as shown in Fig. 9. After 2V, NMOS enters in the saturation region where no further modification in the output frequency is possible. This provides a window of 0.5V for the sensor node for calibration. On the other hand, the output spiking frequency for the given neuron circuit ranges from 15MHz to 30MHz. The circuit diagram of a single synaptic connection between the presynaptic and postsynaptic neuron is shown in Fig 18.

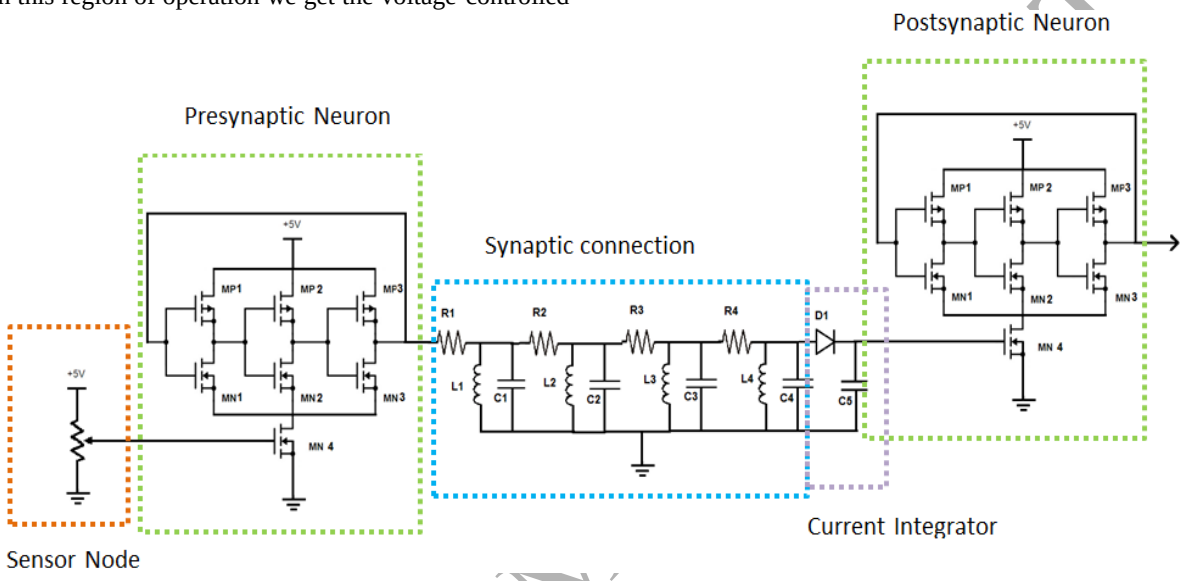

Figure 18. Circuit diagram of a single synaptic connection between the presynaptic and postsynaptic neuron

The circuit diagram for synaptic connection shows a single link from the network diagram shown in Fig 14. The sensor node is shown as a variable resistor (rheostat). For the presynaptic and postsynaptic neuron, the models described in section *V.A* are utilized. For synaptic connection we have utilized an analogue passive 8th order bandpass filter (shown in blue dotted box labeled as synaptic connection). This will provide high Q-factor for the filtering operation performed by the synaptic connection. The circuit for 2nd order bandpass filter comprises of *R1* (resistor), *L1* (inductor) and *C1* (capacitor) which is similar to the synaptic connection model discussed in section *V.B*. Similar 2nd order filters are cascaded comprising components from *R2*, *L2* and *C2* to *R4*, *L4* and *C4* to form an 8th order bandpass filter. The bandpass filter unit is followed by a current integrator unit (shown in purple dotted box labeled as Current Integrator). The current integrator unit comprises of a diode, *D1*, and a capacitor, *C5*. The basic purpose of this unit is to convert the sinusoidal waveform, output from the bandpass unit, to DC voltage value which can be feed to the input node of postsynaptic neuron. Last block is the postsynaptic neuron. The response of the network is collected from the fanout of the postsynaptic neurons.

The transfer function of bandpass filters is set according to the spiking frequencies listed in Table I. In this context, four distinct frequencies have been selected which represents input values applied as stimulus to presynaptic neuron. The values selected as input represents four distinct sensor node values as shown in Fig 15, against the frequency values output by the presynaptic neuron as listed in Table I.

TABLE I. AN INPUT/OUTPUT TABLE FOR PROPOSED NEURON MODEL

S #	Selected Input / Output values	
	Input DC value (in volts)	***Output Spiking Frequency (in MHz)***
1	1.36	23
2	1.38	25
3	1.42	28
4	1.47	34

The transfer function of four bandpass filters shown in the network diagram of Fig. 14 is set in accordance with the frequency values listed in Table I. Discrete electronic implementation is carried out for the proposed circuit. The results were observed on a digital oscilloscope. The output of presynaptic neuron is shown in Fig. 19.

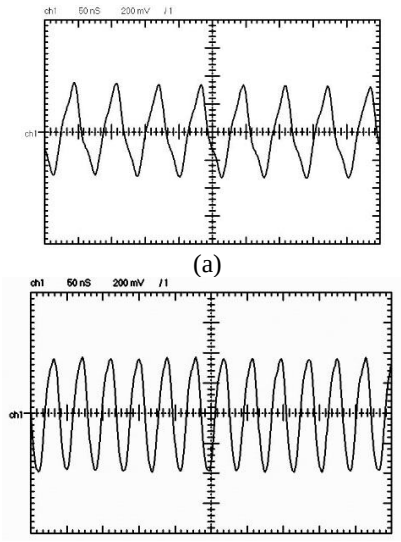

Figure 19. Output of presynaptic neuron with (a) 15 MHz output (input voltage = 1.29V) and (b) 24 MHz output (input voltage = 1.4V)

The results in Fig. 19 clearly indicate that the presynaptic neuron is functioning in accordance with the design requirement that is converting a DC input value into an output oscillating frequency. An input value of 1.42V is applied as test input to the presynaptic neuron that is meant to trigger postsynaptic neuron 3. The output waveform, from the bandpass fiter section, with passband frequency wave and attenuated stopband frequency wave is shown in Fig. 20.

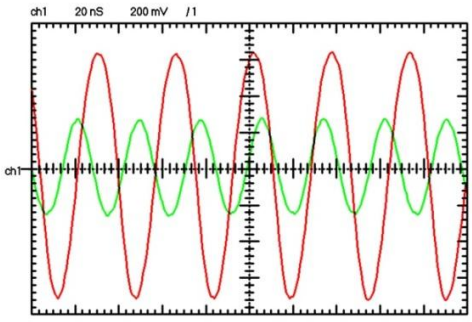

Figure 20. Output of bandpass filter section (red curve) output wave with center frequency of 28 MHz (green curve) attenuated wave at center frequency of 33 MHz

The output of the bandpass filter is observed at the synaptic junctions connected to postsynaptic neurons 2 & 3 with green and red curves, respectively. It clearly shows that the output of synaptic junction for postsynaptic neuron 3 is passed with minor attenuation whereas the output of synaptic junction for postsynaptic neuron 2 is attenuated for more than 50 percent of actual input. These outputs will pass through the integrator blocks and then to the postsynaptic neurons. The output from the postsynaptic neuron 2 and 3 are shown in Fig. 21. The stimulus selected is 1.42V. This will generate an output frequency of 28 MHz from presynaptic neuron and will ultimately force neuron 3 to trigger while there is no response from other postsynaptic neurons.

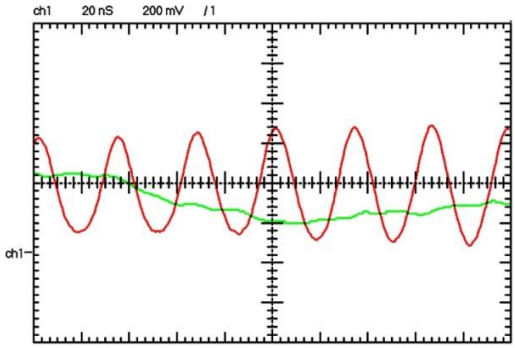

Figure 21. Output of postsynaptic neuron 2 (green curve) and 3 (red curve)

The results shown in Fig. 21 shows that the stimulus that was encoded by the presynaptic neuron is decoded with varied response of postsynaptic neurons. A single neuron triggering from the postsynaptic ensemble (triggering of post synaptic neuron 3 only) is the representation of distinct response of a population when presented with any particular analog input value read by the sensor node.

In order to test the performance of system in 'noisy' environment, a signal that contains noise e^* as expressed in Eq. 7 is applied to the presynaptic neuron. According to Table 1, input DC values feed through sensor represents distinct addressable stimuli θ in the environment. The distance between these DC values can be considered as d mentioned in Eq. 8. The minimum distance is '200mV' between first and second input values listed in Table 1. Following the constraint mentioned in Eq. 8, the error value must be greater than '150mV' in order to misclassify stimulus θ_i. An error value of '20mV' is induced in the signal and output waveforms at the synaptic connection are shown in Fig. 22.

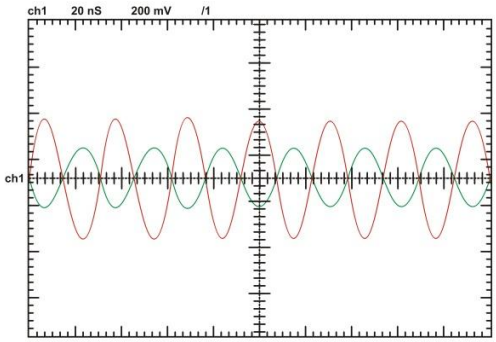

Figure 22. Red curve shows output of synaptic junction of postsynaptic neuron 2 and green curve shows the output at synaptic junction of postsynaptic neuron 1 where the correct output should be the triggering of postsynaptic neuron 2.

Here the synaptic junction of postsynaptic neuron 2 slightly attenuates the input due to inclusion of noise. The noise has negligent impact on the performance of the network due to sigmoidal transfer function of bandpass filter which is realized as a synaptic connection in this model. Any noise value e^* which is below *d/2* will not have an impact on the classification, however, e^* greater than *d/2* will lead to misclassification of input data.

VIII. CONCLUSION

In this paper an efficient method is presented in terms of area and computational effort to embed population coding in neuromorphic hardware as compared to LSHDI mechanism which requires a large number of hidden layer neurons. This mechanism completely avoids hidden layer by embedding non-linear transfer function into the synaptic connections. It has been shown that the presented network model has the capability to embed population coding in neuromorphic hardware. Furthermore, the presented model offers similar selective triggering (winner) mechanism offered by WTA without employing any additional circuitry. A direct relationship between the neurophysiological models and the presented model is created. It has been explained that the synaptic junction in the biological nervous system do perform bandpass filtering operation. Similar bandpass filtering operation is utilized to implement synaptic connections in this model.

This paper also addresses number of questions regarding implementation issues of population coding in neuromorphic hardware. These issues include role of a rate neuron in the context of neuromorphic hardware. This issue has been addressed by using the spiking rate of a neuron as parameter to trigger distinct neurons in the postsynaptic layer. The variation of ISI has also been addressed as a mechanism to embed stimulus information into spiking frequency by the rate neuron and how it can be decoded in the same environment by making synaptic junction resonance aware. It has also been shown that how information contents regarding any stimulus read by the sensor, is transmitted between different neuron layers. The population vector basically decodes the information about stimulus by selectively triggering neurons in the ensemble. This paper also highlights the interface between two rate-encoding neurons.

The role of tuning curve is also discussed by considering it as a function of selective filtering by the synaptic connection. In conventional approaches external parameters are used to embed tuning curve in the hardware such as tanh function for TAB framework. This paper demonstrates the direct implementation of a tuning curve as a transfer function of a bandpass filter.

There are no external parameters applied to the network model presented in this paper. This approach makes the presented network, a standalone system that does not require lengthy calibration procedure. There is no requirement to deploy additional circuitry for WTA algorithm. The inherent structure of the network enforces it to selectively trigger a single postsynaptic neuron to trigger at the output with maximum frequency.

REFERENCES

[1] Mead CA. Analog VLSI and Neural Systems. Reading MA: Addison Wesley; 1989.

[2] Mahowald M, Douglas R. A silicon neuron. Nature. 1991 Dec 19;354(6354):515-8.

[3] Indiveri G, Chicca E, Douglas RJ. Artificial cognitive systems: from VLSI networks of spiking neurons to neuromorphic cognition. Cognitive Computation. 2009 Jun 1;1(2):119-27.

[4] Yu T, Sejnowski TJ, Cauwenberghs G. Biophysical neural spiking, bursting, and excitability dynamics in reconfigurable analog VLSI. IEEE transactions on biomedical circuits and systems. 2011 Oct;5(5):420-9.

[5] Indiveri G, Linares-Barranco B, Hamilton TJ, Van Schaik A, Etienne-Cummings R, Delbruck T, Liu SC, Dudek P, Häfliger P, Renaud S, Schemmel J. Neuromorphic silicon neuron circuits. Frontiers in neuroscience. 2011 May 31;5:73.

[6] Renaud S, Tomas J, Lewis N, Bornat Y, Daouzli A, Rudolph M, Destexhe A, Saïghi S. PAX: A mixed hardware/software simulation platform for spiking neural networks. Neural Networks. 2010 Sep 30;23(7):905-16.

[7] Brüderle D, Petrovici MA, Vogginger B, Ehrlich M, Pfeil T, Millner S, Grübl A, Wendt K, Müller E, Schwartz MO, De Oliveira DH. A comprehensive workflow for general-purpose neural modeling with highly configurable neuromorphic hardware systems. Biological cybernetics. 2011 May 1;104(4-5):263-96.

[8] Furber SB, Lester DR, Plana LA, Garside JD, Painkras E, Temple S, Brown AD. Overview of the SpiNNaker system architecture. IEEE Transactions on Computers. 2013 Dec;62(12):2454-67.

[9] Choudhary S, Sloan S, Fok S, Neckar A, Trautmann E, Gao P, Stewart T, Eliasmith C, Boahen K. Silicon neurons that compute. InInternational Conference on Artificial Neural Networks 2012 Sep 11 (pp. 121-128). Springer Berlin Heidelberg.

[10] Merolla P, Arthur J, Akopyan F, Imam N, Manohar R, Modha DS. A digital neurosynaptic core using embedded crossbar memory with 45pJ per spike in 45nm. In 2011 IEEE custom integrated circuits conference (CICC) 2011 Sep 19 (pp. 1-4). IEEE.

[11] Sharad M, Augustine C, Panagopoulos G, Roy K. Proposal for neuromorphic hardware using spin devices. arXiv preprint arXiv:1206.3227. 2012 Jun 14.

[12] Pickett MD, Medeiros-Ribeiro G, Williams RS. A scalable neuristor built with Mott memristors.Nature materials. 2013 Feb 1;12(2):114-7.

[13] Gehlhaar J. Neuromorphic processing: a new frontier in scaling computer architecture. ACM SIGPLAN Notices. 2014 Apr 5;49(4):317-8.

[14] Papanikolaou A, Wang H, Miranda M, Catthoor F, Dehaene W. Reliability issues in deep deep submicron technologies: time-dependent variability and its impact on embedded system design. InVLSI-SoC: Research Trends in VLSI and Systems on Chip 2008 (pp. 119-141). Springer US.

[15] Song S, Miller KD, Abbott LF. Competitive Hebbian learning through spike-timing-dependent synaptic plasticity. Nature neuroscience. 2000 Sep 1;3(9):919-26.

[16] Bi GQ, Poo MM. Synaptic modifications in cultured hippocampal neurons: dependence on spike timing, synaptic strength, and postsynaptic cell type. The Journal of neuroscience. 1998 Dec 15;18(24):10464-72.

[17] Haykin SS. Neural networks: a comprehensive foundation. Tsinghua University Press; 2001.

[18] Seung HS, Sompolinsky H. Simple models for reading neuronal population codes. Proceedings of the National Academy of Sciences. 1993 Nov 15;90(22):10749-53.

[19] Sparks D. Population coding of saccadic eye movements by neurons in the superior colliculus. Nature. 1988 Mar;332:357-60.

[20] Pouget A, Dayan P, Zemel R. Information processing with population codes. Nature Reviews Neuroscience. 2000 Nov 1;1(2):125-32.

[21] Paradiso MA. A theory for the use of visual orientation information which exploits the columnar structure of striate cortex. Biological cybernetics. 1988 Jan 1;58(1):35-49.

[22] Averbeck BB, Latham PE, Pouget A. Neural correlations, population coding and computation. Nature Reviews Neuroscience. 2006 May 1;7(5):358-66.

[23] Kang K, Shapley RM, Sompolinsky H. Information tuning of populations of neurons in primary visual cortex. The Journal of neuroscience. 2004 Apr 14;24(15):3726-35.

[24] Georgopoulos AP, Carpenter AF. Coding of movements in the motor cortex. Current opinion in neurobiology. 2015 Aug 31;33:34-9.

[25] Theunissen FE, Miller JP. Representation of sensory information in the cricket cercal sensory system. II. Information theoretic calculation of system accuracy and optimal tuning-curve widths of four primary interneurons. Journal of Neurophysiology. 1991 Nov 1;66(5):1690-703.

[26] Pasupathy A, Connor CE. Population coding of shape in area V4. Nature neuroscience. 2002 Dec 1;5(12):1332-8.

[27] Hodgkin AL, Huxley AF. Propagation of electrical signals along giant nerve fibres. Proceedings of the Royal Society of London. Series B, Biological Sciences. 1952 Oct 16:177-83.

[28] Sherman SM. Tonic and burst firing: dual modes of thalamocortical relay. Trends in neurosciences. 2001 Feb 1;24(2):122-6.

[29] Oswald AM, Doiron B, Maler L. Interval coding. I. Burst interspike intervals as indicators of stimulus intensity. Journal of Neurophysiology. 2007 Apr 1;97(4):2731-43.

[30] Thakur CS, Hamilton TJ, Wang R, Tapson J, van Schaik A. A neuromorphic hardware framework based on population coding. In 2015 International Joint Conference on Neural Networks (IJCNN) 2015 Jul 12 (pp. 1-8). IEEE.

[31] Izhikevich EM. Dynamical systems in neuroscience. MIT press; 2007.

[32] Butts DA, Goldman MS. Tuning curves, neuronal variability, and sensory coding. PLoS Biol. 2006 Mar 21;4(4):e92.

[33] Deneve S, Latham PE, Pouget A. Reading population codes: a neural implementation of ideal observers. Nature neuroscience. 1999 Aug 1;2(8):740-5.

[34] Abbott LF, Dayan P. The effect of correlated variability on the accuracy of a population code. Neural computation. 1999 Jan 1;11(1):91-101.

[35] Cover TM, Thomas JA. Elements of information theory. John Wiley & Sons; 2012 Nov 28.

[36] Pao YH, Takefji Y. Functional-link net computing. IEEE Computer Journal. 1992;25(5):76-9.

[37] Schmidt WF, Kraaijveld MA, Duin RP. Feedforward neural networks with random weights. In Pattern Recognition, 1992. Vol. II. Conference B: Pattern Recognition Methodology and Systems, Proceedings., 11th IAPR International Conference on 1992 Aug (pp. 1-4). IEEE.

[38] Huang GB, Zhu QY, Siew CK. Extreme learning machine: theory and applications. Neurocomputing. 2006 Dec 31;70(1):489-501.

[39] Stewart TC, Eliasmith C. Large-scale synthesis of functional spiking neural circuits. Proceedings of the IEEE. 2014 May;102(5):881-98.

[40] Tapson J, Cohen G, Afshar S, Stiefel K, Buskila Y, Wang R, Hamilton TJ, van Schaik A. Synthesis of neural networks for spatio-temporal spike pattern recognition and processing. arXiv preprint arXiv:1304.7118. 2013 Apr 26.

[41] Izhikevich EM, Desai NS, Walcott EC, Hoppensteadt FC. Bursts as a unit of neural information: selective communication via resonance. Trends in neurosciences. 2003 Mar 31;26(3):161-7.

[42] Lisman JE. Bursts as a unit of neural information: making unreliable synapses reliable. Trends in neurosciences. 1997 Jan 31;20(1):38-43.

[43] Izhikevich E.M., Desai N., and Walcott E.C. Subthreshold oscillations and selective interactions in rat brainstem mes V neurons in vitro, manuscript in preparations, 2003.

[44] Markram H, Wang Y, Tsodyks M. Differential signaling via the same axon of neocortical pyramidal neurons. Proceedings of the National Academy of Sciences. 1998 Apr 28;95(9):5323-8.

[45] Fortune ES, Rose GJ. Short-term synaptic plasticity as a temporal filter. Trends in neurosciences. 2001 Jul 1;24(7):381-5.

[46] Fortune ES, Rose GJ. Short-term synaptic plasticity contributes to the temporal filtering of electrosensory information. The Journal of Neuroscience. 2000 Sep 15;20(18):7122-30.

[47] Alex T. Frequency-filtering properties of 'dynamic' cortical synapses and their contributions to the behavior of small networks. Computational Neuroscience (CNS) conference, invited talk, Chicago, July 23, 2002.

[48] Butterworth S. On the theory of filter amplifiers. Wireless Engineer. 1930 Oct;7(6):536-41.

[49] Rabaey JM, Chandrakasan AP, Nikolic B. Digital integrated circuits. Englewood Cliffs: Prentice hall; 2002 Dec.

[50] Miau F, Papageorgiou CS, Itti L. Neuromorphic algorithms for computer vision and attention. InInternational Symposium on Optical Science and Technology 2001 Nov 14 (pp. 12-23). International Society for Optics and Photonics.

[51] Sandamirskaya Y. Dynamic neural fields as a step toward cognitive neuromorphic architectures.

[52] Indiveri G. Neuromorphic VLSI models of selective attention: from single chip vision sensors to multi-chip systems. Sensors. 2008 Sep 3;8(9):5352-75.

[53] Barrows GL, Miller KT, Krantz B. Fusing neuromorphic motion detector outputs for robust optic flow measurement. InNeural Networks, 1999. IJCNN'99. International Joint Conference on 1999 (Vol. 4, pp. 2296-2301).

Saad Qasim Khan graduated from the N.E.D University of Engineering and Technology, Karachi, Pakistan in Computer and Information Systems Engineering in 2009 and subsequently completed his Masters of Engineering in Computer Systems Engineering from the same institute in 2013. He is currently pursuing his Ph.D. at the very same institute since 2014, specializing in Neuromorphic hardware design. Currently his research interests include hardware/software neural network implementations, CMOS circuit design, Neuromorphic hardware and computational neuroscience.

He is currently a lecturer at the Department of Computer and Information Systems Engineering, NED University of Engineering and Technology, Karachi, Pakistan.

Arfan Ghani is currently working as a Senior Lecturer (Associate Professor) in Electrical and Electronic Engineering at Coventry University, England. He graduated with Distinction in Electronics Engineering from the NED Engineering University in Pakistan and subsequently completed his Master of Science degree in Electrical Engineering from the Danish Technical University in Copenhagen and Ph.D. in Neural Engineering from the University of Ulster in N. Ireland, UK.
He has worked as a post-doc in Neuroprosthesis Lab at Newcastle University, and University of Ulster, UK. Dr. Ghani has got industrial experience working as ASIC/FPGA designer at Vitesse Semiconductors, Denmark and Intel Research, Cambridge. He is a Chartered Engineer (CEng), Fellow of Higher Academy (FHEA) in the UK and member of IET. He is currently a PI and Co-PI on number of research grants (UK/EU) and his research interests include the biomedical circuits and systems, neuromorphic hardware, optoelectronics, bio-inspired electronic systems, biological signal processing and systems-on-chip design.

Muhammad Khurram was born in Karachi, Pakistan, in 1980. He received the B.E. degree in computer systems engineering and the M.E. degree in computer and information systems engineering from the NED University of Engineering and Technology, Karachi, Pakistan, in 2002 and 2007, respectively. He received the Ph.D. degree in computer systems engineering from Massey University, Albany, Auckland, New Zealand. His research interests include the design of nano-metric RF integrated circuits using state-of-the-art CMOS technologies. He has ten international journal and conference publications.